Crossover from reptation to Rouse dynamics in the cage model

A. Drzewiński[1] and J. M. J. van Leeuwen[2]
[1]*Czestochowa University of Technology, Institute of Mathematics and Computer Science, ul.Dabrowskiego 73, 42-200 Czestochowa, Poland*
[2]*Instituut-Lorentz, Leiden University, P.O. Box 9506, 2300 RA Leiden, The Netherlands*
(Received 12 September 2006; published 1 December 2006)

The two-dimensional cage model for polymer motion is discussed with an emphasis on the effect of sideways motions, which cross the barriers imposed by the lattice. Using the density matrix method as a solver of the master equation, the renewal time and the diffusion coefficient are calculated as a function of the strength of the barrier crossings. A strong crossover influence of the barrier crossings is found and it is analyzed in terms of effective exponents for a given chain length. The crossover scaling functions and the crossover scaling exponents are calculated.

DOI: 10.1103/PhysRevE.74.061801 PACS number(s): 61.25.Hq, 05.10.−a, 83.10.Kn

I. INTRODUCTION

The motion of a single polymer dissolved in a gel has been described in terms of reptation [1]. Typical for reptation is that the polymer chain moves inside a tube, which can only be refreshed by growth and shrinkage at the ends. In order to make this motion suitable for analysis, lattice models have been designed of which the cage model, proposed by Edwards and Evans in 1981 [2], is the oldest. It was mainly considered as a simple model for reptation [1,3], which is indeed the main mode of motion for polymers dissolved in a gel. The embedding lattice plays the role of the gel imposing barriers for the motion. The original introduction allowed for two types of motion: "reptations," which are motions along the confining tube and sideways motions or "barrier crossings," in which the chain overcomes a barrier and thus changes the tube configuration. So far most attention has been paid to the reptations only. In this paper we concentrate on the interplay, which is quite delicate, as we will show. For example, naively one might think that the diffusion coefficient is the linear sum of the contributions of the two mechanisms, but that is not at all the case, as has been noted by Klein Wolterink and Barkema [4] in a similar context. This makes it difficult to analyze experiments in which the simultaneous presence of the two types of motion can never be excluded. In the cage model the interplay of the two modes can be fully analyzed.

The model has extensively been studied by Monte Carlo simulations, which seems to be the only way to deal with the master equation for the stochastic motion [5–9]. Since the relevant master equation does not obey detailed balance, no systematic solution method exists. The issues, to which we presently address ourselves, were the subject of a lively debate in the early nineties. The various simulations showed certain tendencies, but the limitation to fairly short chains and the intrinsic statistical noise prevented in our opinion definite settling the role of Rouse dynamics vs reptation.

In this paper we use an alternative method, based on the analogy between the master equation and the Schrödinger equation, by which the temporal evolution of the probability distribution of the chain configurations corresponds to the evolution of the wave function. Of course the wave function may be complex, while the probability distribution is real and positive. Also the master operator, viewed as a Hamiltonian, is non-Hermitian, which implies decay towards the stationary state in contrast to the oscillatory temporal behavior of the eigenfunctions of quantum problems. In spite of these differences, one can benefit from the analogy, the more so because the master operator corresponds to the Hamiltonian of a one-dimensional spin chain, for which the very efficient density matrix method (DMRG) has been designed by White [10]. The cage model remains a one-dimensional quantum problem, irrespective of the lattice in which it is embedded, because the chain itself is a linear structure.

We focus on two dynamic properties: the renewal time τ and the diffusion coefficient D, and determine them directly from the master operator. Both properties refer to asymptotically long times (the stationary state) and thus our calculations are complementary to the Monte Carlo simulations which probe the short and intermediate time behavior [11]. The renewal time is the time needed for the chain to assume a new configuration, which has no memory of the original one. It is found from the gap in the spectrum of the master operator. The master equation always has a trivial eigenvalue 0, corresponding to the stationary state. Any other initial state ultimately decays towards the stationary state and the slowest relaxation time (the inverse of the gap) is the renewal time. Its calculation is difficult because for long chains, the gap becomes very small and the excited states are hard to disentangle from the stationary state. In fact the gap decays with a negative power z of the length N of the chain, such that $\tau \sim N^z$. The zero-field diffusion coefficient D is related to the drift velocity in a weak driving field. It decays as a power N^{-x}.

We will confine ourselves to one- and two-dimensional embeddings. The degree of difficulty of the solution is related to the dimension of the embedding lattice, simply because the higher the embedding dimension, the higher the spin in the corresponding spin chain and the more states required in the DMRG approximation. In this paper we will show that the one-dimensional version, which is admittedly unrealistic, allows an analytical solution. The two-dimensional embedding lattice presents the problem already in its full complexity, while of course the three-dimensional case is of the most experimental relevance. Actually the uni-

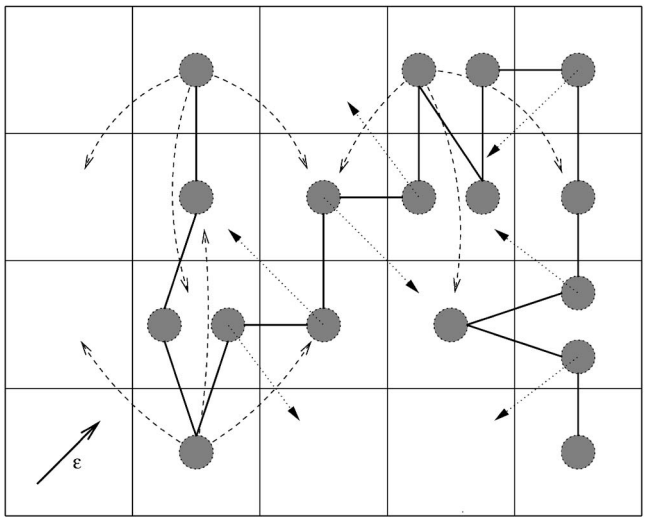

FIG. 1. A picture of the polymer chain, consisting of reptons (gray dots) and some examples of allowed repton motions. The dashed arrows denote reptations (hernia moves), whereas the dotted ones represent barrier crossings. The solid arrow presents the driving field direction.

versal properties are believed to be the same for embedding lattices from $d=2$ and higher. The practical limitation to two-dimensional embedding lattices derives from the fact that our computations are already at the limits of present day possibilities.

The DMRG approach yields very accurate results in the domain where it converges. This enables us to use finite-size scaling analysis for the determination of the exponents and the crossover scaling functions. The case without crossing barriers (the reptation dynamics) has powers different from the case with these crossings (Rouse dynamics). From the viewpoint of dynamic scaling, the exponents are exotic and good illustrations of how crossover takes places from one type of behavior to another. A crossover scaling representation for τ and D strongly elucidates their behavior.

II. THE MODEL

The model is a chain of $N+1$ reptons, connected by N links $(y_1,\ldots,y_N)$ to neighboring cells of a hypercubic lattice. A picture of a chain is given in Fig. 1. The mobile units are the reptons. The y_i can take $2d$ values and because we have a two-dimensional embedding lattice, we can denote them by the directions N (north), E (east), S (south), and W (west). Two consecutive reptons are always in adjacent cells, but the chain may backtrack and cells can be multiply occupied (see Fig. 1). The y_i variables characterize the chain, since the absolute position is irrelevant for the properties that we consider. The statistics of the model is governed by the master equation for the probability distribution $P(\mathbf{Y},t)$, where $\mathbf{Y}$ stands for the complete configuration $(y_1,\ldots,y_N)$. It has the general form

$$\frac{\partial P(\mathbf{Y},t)}{\partial t} = \sum_{\mathbf{Y}'} [W(\mathbf{Y}|\mathbf{Y}')P(\mathbf{Y}',t) - W(\mathbf{Y}'|\mathbf{Y})P(\mathbf{Y},t)] \equiv \sum_{\mathbf{Y}'} M(\mathbf{Y},\mathbf{Y}')P(\mathbf{Y}',t). \quad (1)$$

The W's are the transition rates of the possible motions that we have indicated in Fig. 1. The matrix M combines the gain terms (in the off-diagonal elements) and the loss terms (on the diagonal). M is a sum of matrices, for each repton one,

$$M(\mathbf{Y},\mathbf{Y}') = \sum_{i=0}^{N} M_i(\mathbf{Y},\mathbf{Y}'), \quad (2)$$

where the sum runs over the reptons starting with the tail repton $i=0$ to the head repton $i=N$. The tail repton matrix is diagonal in all the link variables except the first,

$$M_0(\mathbf{Y},\mathbf{Y}') = m_0(y_1|y_1') \prod_{i=2}^{N} \delta_{y_i,y_i'}. \quad (3)$$

The tail repton produces exclusively reptations. Each move of the tail repton can be seen as a combination of a withdrawal towards the cell of the next repton and from thereon a move to a new cell. The matrix m_0 is explicitly given by the scheme

$y\backslash y'$	N	E	S	W
N	$-1-2B^2$	1	B^{-2}	B^{-2}
E	1	$-1-2B^2$	B^{-2}	B^{-2}
S	B^2	B^2	$-1-2B^{-2}$	1
W	B^2	B^2	1	$-1-2B^{-2}$

The parameter $B=\exp(\epsilon/2)$ is a bias, which accounts for the influence of a driving field, which can be an electric field when the reptons are charged. The value of (the small) ϵ is a dimensionless measure for the strength of this driving field. The driving field is along the body diagonal, here in the north-east direction. So if the link N moves to the direction W, the tail repton moves two units in the direction of the field. The reverse process gets a bias B^{-2}. The head repton transition probabilities are given by a similar matrix with B^2 replaced by B^{-2}. They are depicted in Fig. 2. One could give all the transitions an overall factor, but this would only influence the overall time rate. So we keep the unbiased transitions equal to 1.

The internal repton i changes two consecutive links y_i, y_{i+1}. The matrix M_i is diagonal in all the other link variables. The transition matrix contains two types of contributions:

(i) *Reptations.* These are the cases where y_i' and y_{i+1}' are opposite, e.g., N and S (sometimes called a hernia in the chain). Then repton i can retract to the cell to which it is doubly connected and then recreate a new hernia, a new pair of opposite links, e.g., E and W (see Fig. 3). Note that the sequence EW differs from WE. Moves towards EW and WE obtain different biases.

(ii) *Barrier crossings.* A typical case is the sequence NE. It may flip to the sequence EN. To reach that new position it

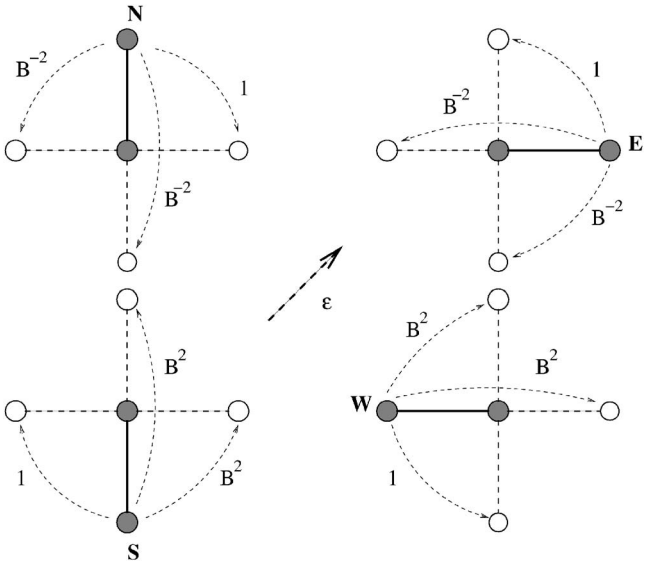

FIG. 2. The allowed motions of the head repton with corresponding transition ratios. The dashed arrow presents the driving field.

necessarily has to cross the lattice point enclosed by the two sequences. We give these transitions a (small) factor c together with the biases which measure the distance that repton i travels in the direction of the field (see Fig. 4).

It is worth noticing that for the cage model all transition ratios are proportional to the bias B^2 (or B^{-2}) [12].

Generally, conservation of probability follows from the fact that the sum over the columns of the matrix M vanishes. So M has a zero eigenvalue and the eigenfunction corresponding to this eigenvalue is the stationary state of the system, to which every other initial state ultimately decays. The matrix is nonsymmetric, due to the bias, which gives different rates to a process and its inverse. Thus one has to distinguish between left and right eigenfunctions. The left eigenfunction, belonging to the zero eigenvalue, is trivial (all components equal), and the right eigenfunction is the stationary state distribution.

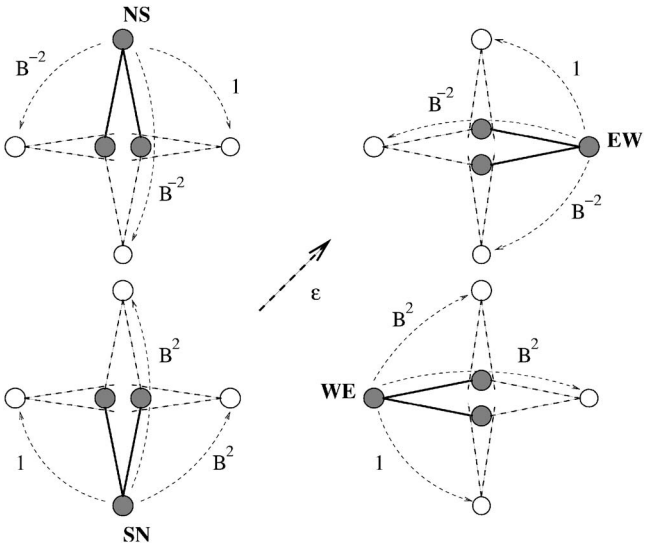

FIG. 3. The allowed motions of the hernia with corresponding transition ratios. The dashed arrow presents the driving field.

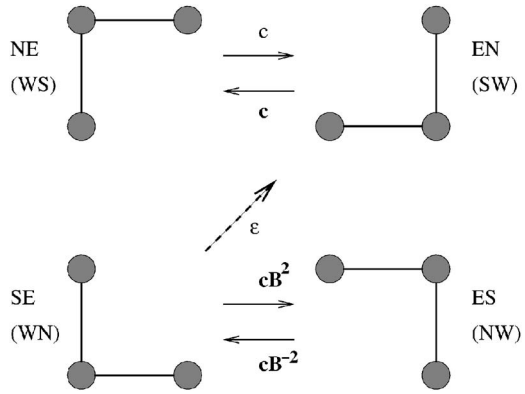

FIG. 4. The solid arrows present allowed motions for the barrier crossing with corresponding transition ratios. The dashed arrow presents the driving field.

The renewal time is usually defined for bias $B=1$ (no driving field). For the diffusion coefficient we introduce a small driving field which induces an overall drift $v_d \sim \epsilon$. The proportionality coefficient gives the diffusion coefficient D according to the Einstein relation

$$D = \frac{1}{N}\left(\frac{\partial v_d}{\partial \epsilon}\right)_{\epsilon=0}. \tag{4}$$

$M(\mathbf{Y},\mathbf{Y}')$ is the matrix representation of the master operator $\mathcal{M}$, acting as a Hamiltonian. As M is nonsymmetric the Hamiltonian $\mathcal{M}$ is non-Hermitian. One may view the states y_i of the links as the states of a discrete plane rotator. However, translating the action of $\mathcal{M}$ in terms of rotator operators does not lead to a more transparent expression (except for $d=1$, which maps on a spin 1/2 chain, see Sec. IV).

The model has only a few parameters: the length of the chain N, the strength of the driving field ϵ, and the relative strength c of the barrier crossings with respect to the reptating transitions. Experimentally the most interesting combination is the case where $\epsilon \to 0$ and $N \to \infty$. This is a delicate limiting process since the product ϵN may stay finite and influences the nature of the stationary state strongly. The properties that we consider, renewal time τ and diffusion coefficient D, refer to the case where this product remains infinitesimal. Thus effectively we have only N and c as parameters. We will also see in this pair interesting scaling combinations occur.

III. SYMMETRIES OF THE MASTER OPERATOR

For our analysis optimal use of the symmetries of the master operator is vital. We have chosen the driving field in the north-east direction in order to make the directions N and E as well as S and W equivalent. We use two symmetry operations of the lattice:

(i) Reflection with respect to the field axis. This turns the direction N into E and vice versa and similarly it interchanges S and W. We refer to this operation as $\mathcal{S}_\perp$.

(ii) Reflection parallel to the field axis, which interchanges the directions N and W as well as E and S. It is denoted as $\mathcal{S}_{\|}$.

The Hamiltonian is invariant under the operation $\mathcal{S}_{\perp}$ but not under $\mathcal{S}_{\|}$; it would be, if it were accompanied by a field inversion. We can analyze the consequences of the symmetry by considering the following transformation

$$\begin{pmatrix} 0 \\ 1 \\ 2 \\ 3 \end{pmatrix} = \mathcal{R} \begin{pmatrix} N \\ E \\ S \\ W \end{pmatrix} = \frac{1}{2} \begin{pmatrix} N+E+S+W \\ N-E+S-W \\ N+E-S-W \\ N-E-S+W \end{pmatrix}. \tag{5}$$

$\mathcal{R}$ is an orthogonal transformation of the states N, E, S, and W of the links. The new states have a definite symmetry character under the two operations. The state 0 is even under $\mathcal{S}_{\perp}$ and $\mathcal{S}_{\|}$, the state 1 is odd and even, 2 is even and odd, and 3 is odd for both. Let us illustrate the effect of this rotation by applying it to the matrix m_0, yielding

$$\mathcal{R} m_0 \mathcal{R}^{-1} = \begin{pmatrix} 0 & 0 & 0 & 0 \\ 0 & m_{11} & 0 & m_{13} \\ m_{20} & 0 & m_{22} & 0 \\ 0 & m_{31} & 0 & m_{33} \end{pmatrix}. \tag{6}$$

The entries are now labeled by the states 0, 1, 2, and 3 and are given by

$$m_{11} = -2 - (B^2 + B^{-2}) = m_{33}, \quad m_{22} = -2(B^2 + B^{-2}),$$

$$m_{20} = -2(B^2 - B^{-2}) = 2m_{31} = 2m_{13}. \tag{7}$$

One sees that the matrix is block diagonal with a 2×2 matrix in the $0-2$ channel and one in $1-3$ channel. This results from the invariance of the Hamiltonian with respect to $\mathcal{S}_{\perp}$, since the states 0 and 2 are even and the states 1 and 3 are odd under this symmetry. So states of different parity under $\mathcal{S}_{\perp}$ are not mixed by the Hamiltonian. One also observes that the matrix becomes diagonal for $B=1$. The off-diagonal elements concern transitions where the symmetry under field inversion is changed.

The symmetry character of the links in the new states can be carried over to larger segments of the chain, simply by multiplying the parities of the constituting links. The states 0, 1, 2, and 3 not only function as states of the links, but also as indices for the four different symmetry classes. What has been shown in detail for the tail repton holds also for the total Hamiltonian. It is invariant under $\mathcal{S}_{\perp}$ and for $B=1$ also under $\mathcal{S}_{\|}$.

For the diffusion coefficient we expand the master equation in powers of ϵ.

$$\mathcal{M} = \mathcal{M}_0 + \epsilon \mathcal{M}_1 + \cdots, \quad P(\mathbf{Y}) = P_0(\mathbf{Y}) + \epsilon P_1(\mathbf{Y}) + \cdots, \tag{8}$$

and obtain the equations

$$\mathcal{M}_0 P_0 = 0, \quad \mathcal{M}_0 P_1 = -\mathcal{M}_1 P_0. \tag{9}$$

The first equation is trivially fulfilled by a constant $P_0(\mathbf{Y})$, since the matrix M_0 is symmetric and the right eigenvector becomes equal to the trivial left eigenvector. Note that $P_0(\mathbf{Y})$ is the direct product of state 0 for all the links. When we perform the rotation (5) on all links, the vector P_0 changes from a constant in all entries into the vector with a 1 in the first entry and a 0 in all others.

The second equation is a set of homogeneous linear equations for the components of $P_1(\mathbf{Y})$. It is soluble, since the right-hand side of the equation is perpendicular to the left eigenvalue (which remains true for all orders in ϵ). So we can make the solution definite by requiring that it is also orthogonal to the trivial left eigenvector. $P_1(\mathbf{Y})$ yields the lowest order drift velocity v_d.

From the viewpoint of symmetries, the operator $\mathcal{M}_0$ is invariant with respect to both $\mathcal{S}_{\perp}$ and $\mathcal{S}_{\|}$. So it does not affect the symmetry character of P_1, which therefore inherits its symmetry from the right-hand side of Eq. (9). The latter derives its symmetry from $\mathcal{M}_1$ since P_0 is fully symmetric. From the example (6) we can see what the tail-repton Hamiltonian does to the first link: it turns it from state 0 (the building block of P_0) to state 2. Detailed calculations show that this also holds for the other components of $\mathcal{M}_1$. By $\mathcal{M}_1$ the vector P_0 turns from sector 0 to sector 2. This is not surprising since closer inspection of the right-hand side of Eq. (9) shows that it is the microscopic expression for the drift velocity. This reverses sign under $\mathcal{S}_{\|}$ but stays invariant under $\mathcal{S}_{\perp}$, which is indeed the symmetry character of sector 2.

IV. THE ONE-DIMENSIONAL MODEL

As a curiosity we mention the cage model for a one-dimensional embedding lattice. Then the y_i can take only two values, which one would naturally take as 1 and -1. 1 is a step forward and -1 a step backward along the embedding line. On the line there is no possibility of barrier crossing and we have therefore only reptations. An internal move takes place when a pair of links $(1,-1)$ turns into $(-1,1)$ or vice versa. In addition the tail and head link can change from 1 to -1 or from -1 to 1. Such a model belongs to the class of models which can be solved by the matrix product representation designed by Derrida *et al.* [13]. Usually the model is discussed in terms of the variables 1 (a particle) and 0 (a vacancy) and one visualizes the dynamics as a form of traffic. The particles cannot overtake each other and have to wait until they can exchange with a vacancy. The mutual exclusion of particles corresponds in the cage model to the fact that a repton cannot move when it is surrounded by two links of the same value. At the ends of the chain particles enter and leave with certain rates, which in the cage model means that the tail (and head) link can change into their opposite direction. Comparing the rules by which 1 and -1 can interchange in the cage model and the rates at which 1's and -1's are created at the head and tail of the chain, one finds the rules for the equivalent traffic model.

The class of such traffic models has been solved by Sasamoto [14] and independently by Blythe *et al.* [15]. In [16] this model has been related to the necklace model for reptation, where the results of the traffic model are formulated in terms of the language of polymer motion and expres-

sions are derived for the drift velocity and the diffusion coefficient. It is interesting that one has a solution for the whole range of values of the bias B. For example, the value of the drift velocity becomes independent of the length N and reads for large N

$$v_d \simeq \frac{1}{4}(B - B^{-1}). \tag{10}$$

Thus indeed for small ϵ the drift velocity becomes proportional to ϵ. The diffusion coefficient follows using Eq. (4) with an asymptotic decay as $D \sim N^{-1}$ and the diffusion exponent equals $x=1$.

Not only the gap can be calculated explicitly, but also the whole spectrum of the zero field Hamiltonian, since it becomes equivalent with the Heisenberg ferromagnetic spin chain. The gap Δ reads

$$\Delta = -2[1 - \cos(\pi/N)]. \tag{11}$$

Note that the gap vanishes as $\Delta \sim N^{-2}$ for long chains, yielding $z=2$.

Although all the moves of the $d=1$ cage model are reptations, the exponents for the gap and the diffusion coefficient are not typical for reptation. The reason is that the one-dimensional model has no obstacles which slow down the motion by an order of magnitude in the chain length N, as is characteristic for reptation.

V. EFFECTIVE EXPONENTS AND CONVERGENCE

The DMRG expands the solution of the master equation in a basis of size m. The accuracy of the method can be tested by an internal parameter: the truncation error [10], but more convincingly by the convergence of the results as function of m. The method is variational and m is the size of the space of variational parameters. In Ref. [17] we have discussed the technique of the DMRG method in relation to the master equation for reptation models. A log-log plot of the raw data for the gap as a function of chain length N is not very revealing, but rather misleading, as has been pointed out by Carlon *et al.* [18]. A much more refined way of analyzing the data is to use effective exponents. For the gap we define

$$z_N = \frac{\ln \tau(N+1) - \ln \tau(N-1)}{\ln(N+1) - \ln(N-1)} \simeq \frac{d \ln \tau}{d \ln N}, \tag{12}$$

which is a function of the chain length. If the renewal time were a strict power law $\tau \sim N^z$, the expression (12) would equal z, independent of N. We want to stress that only very smooth data can be used to calculate these effective exponents, because noise, which is, e.g., inherent in simulations, will magnify in the ratio of small differences.

In order to obtain an estimate of the convergence we give in Fig. 5 two sets of curves for $c=0.01$ and $c=0$ for various m. The curves for $c=0.01$ are quite close, such that further increase of m does not lead to significantly different results. On the contrary, for the pure reptation case $c=0$, the curves keep changing with m for longer and longer chains. Note that the basis is already unusually large ($m=180$) for DMRG calculations. The large m was possible due to the speed up of

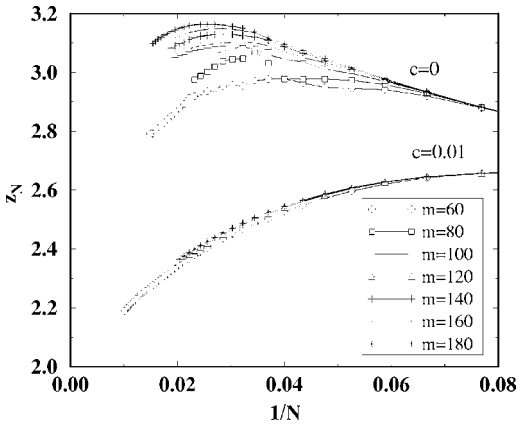

FIG. 5. Comparison of m dependence for the gap exponent at zero and nonzero c.

the process by using the full symmetry of the lattice. The double symmetry allowed one to enlarge the size of the basis m by a factor 4. For each value of c there is a maximal value of N for which the results converge for feasible values of m. Within that range the DMRG values are also sufficiently accurate such that the small differences in Eq. (12) do not suffer from computational noise. In the pictures of the coming sections we only plot the data which do not depend on the value of m.

For the diffusion coefficient the domain of m-independent data is even more restricted. Here we introduce, similar to (12), the effective diffusion exponent

$$x_N = -\frac{\ln D(N+1) - \ln D(N-1)}{\ln(N+1) - \ln(N-1)} \simeq -\frac{d \ln D}{d \ln N}. \tag{13}$$

In Fig. 6 we show the exponent x_N for $c=0$ and $c=0.01$. The latter is again reasonably convergent, but for the former we could not go to sufficiently large m such that a convergent domain starts to emerge. One also observes noise which is not visible on a log-log plot, but which shows up as a result of small numbers in numerator and denominator in Eq. (13). So practically our calculations are limited to values larger than $c=0.001$.

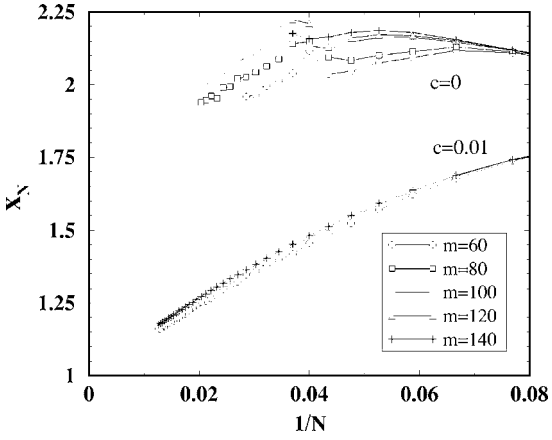

FIG. 6. The comparison of m dependence for the diffusion exponent at $c=0$ and $c=0.01$.

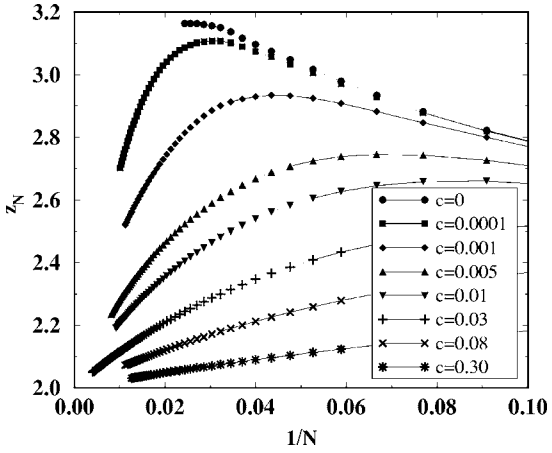

FIG. 7. The renewal time exponent as a function of the length of the chain for various values of the barrier crossing rate c. Note that we have shortened the curve for $c=0$ with respect to the best curve ($m=180$) in Fig. 5, because for longer chains we have significant changes with increasing m.

The local exponents z_N for the renewal time obtained for various c are collected in Fig. 7. In Fig. 8 we plot, in the same way, the local exponent x_N for the diffusion coefficient. Generally, in spite of the above mentioned restrictions, we can make the following observations.

(a) Chains of the order of $N \simeq 100$ are not yet in the asymptotic regime. The effective exponents still deviate appreciably from the asymptotic value. In other words, there are large corrections to scaling. In particular, the plateaus in the small c curves may easily lead to the conclusion that the exponent has settled on a too large value.

(b) The influence of small values of c is quite strong for long chains. We come back on this point when we discuss the crossover behavior.

(c) Although we have no clear evidence that the $c=0$ curve for the gap tends towards the asymptotic value $z_\infty=3$, it is clear that the curves for smaller and smaller c "try" to approach this theoretical value for reptation. The approach to the asymptotic value $z_\infty=2$, for larger c, is evident. This is the exponent for Rouse dynamics.

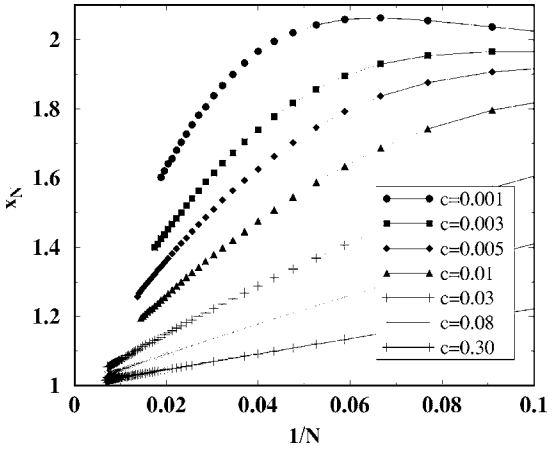

FIG. 8. The diffusion exponent as a function of the length of the chain for various values of the barrier crossing rate c.

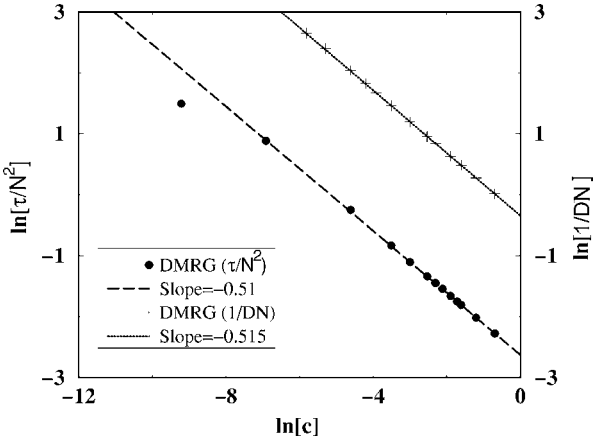

FIG. 9. Log-log plots of the renewal time and the diffusion coefficient as function of c.

(d) The curves that we could calculate for the diffusion coefficient approach the asymptotic exponent $x_\infty=1$, which is again the Rouse exponent for diffusion.

VI. CROSSOVER SCALING

As the curves of Figs. 7 and 8 show, the renewal time τ and the diffusion coefficient D are widely varying functions of the two parameters c and N. We can organize the data more transparently in terms of a crossover scaling function, aiming at data collapse.

Anticipating the asymptotic values of the two regimes $c \to 0$ and a fixed $c \neq 0$, the following representation is adequate for the renewal time:

$$\tau(N,c) = N^3 g(c^\theta N). \tag{14}$$

From such a representation one derives for the effective exponent the expression

$$\frac{d \ln \tau}{d \ln N} = 3 + \frac{d \ln g(c^\theta N)}{d \ln(c^\theta N)}. \tag{15}$$

The crossover function $g(x)$ itself should be expandable for small arguments as

$$g(x) = g_0 + g_1 x + \cdots \tag{16}$$

and for large arguments as

$$g(x) \simeq \frac{1}{x}\left(g_{-1} + \frac{g_{-2}}{x} + \cdots\right). \tag{17}$$

Inserting the asymptotic behavior (17) into Eq. (14) we obtain

$$\ln(\tau/N^2) = \ln g_{-1} - \theta \ln c + \cdots, \tag{18}$$

where the dots refer to corrections of order $1/N$. In Fig. 9 we have made a plot of $\ln(\tau/N^2)$ vs $\ln c$, extrapolated to $N \to \infty$, which corresponds to the first two terms of Eq. (18). As one sees the curve is fairly straight, with a slope $\simeq -0.51$, in the domain where the data are most accurate. We use this value in a scaling plot of $g(x)$, which is shown in Fig. 10. The most

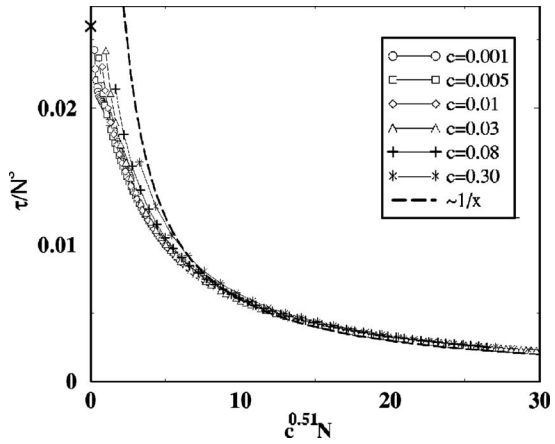

FIG. 10. The crossover function g. The thick cross denotes $g(0)$.

important part of the figure is that for large argument the data collapse and fall on a curve which decays as $1/x$, implying the crossover from reptation to Rouse dynamics. The pure reptation behavior follows from the finiteness of $g(x)$ for small argument. The value $g(0)$ can be derived from a plot of τN^{-3} versus N^{-1}. We find the value $g(0) \simeq 0.026$, which is in good agreement with the behavior of the curves for small argument. We see that the data at small x do not coincide as well as for large x. The reason is the inclusion of small values of N for small c. Here the N is not sufficiently large to have scaling. One should make N larger and c smaller to obtain good scaling in that region, but that regime is as yet inaccesible to us.

In Fig. 9 also $\ln 1/DN$ is plotted as function of $\ln c$. It again gives a straight line with the same slope $\theta \simeq 0.515$. We use this value in the scaling plot, Fig. 11, for the diffusion coefficient in the form

$$D(N,c) = N^{-2} f(c^{\theta} N). \tag{19}$$

As one sees the collapse is amazingly good here in view of the lesser quality of the data, as compared to the renewal time. Also smaller N and "large" c are included, although no real scaling can be expected for these values. It proves that

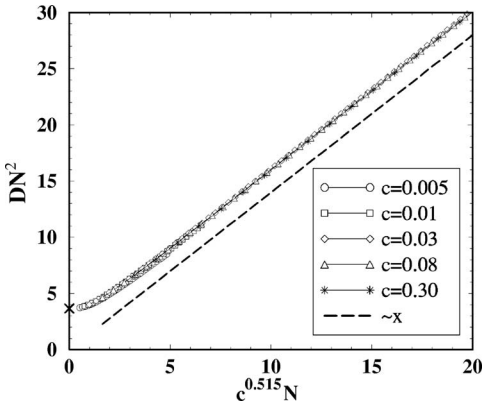

FIG. 11. The crossover function f. The thick cross denotes $f(0)$.

crossover scaling works very well for the diffusion coefficient. The crossover scaling function f approaches again a finite value at $x=0$ that can be estimated from Fig. 11 as $f(0) \simeq 3.67$. For large arguments, $f(x)$ should behave as $f(x \to \infty) \sim x$, which is confirmed by the plot. It again shows the crossover from reptation to Rouse dynamics.

VII. DISCUSSION

We have found that the renewal time and the diffusion coefficient can be transparently described by the crossover scaling functions (14) and (19). In particular the diffusion data fit the scaling curve very well for practically all the points calculated. The crossover scaling exponent is found to be $\theta=0.51$ and we are fairly convinced that the exact value is $1/2$. Not only do the data support this value but also an analytical argument can be given for $\theta=1/2$, which runs as follows: Reptation does not change the backbone of the chain (which results from stripping the hernias from the chain). The hernias walk along the backbone and are created and annihilated at the end of the chain. For the removal of a backbone segment of length N, the end repton has to diffuse over a distance of order N. For this diffusion along the backbone the curvilinear diffusion coefficient applies, which is an order N larger than the total diffusion coefficient, so it is of order N^{-1} (see also Sec. IV). The time scale for diffusion is distance squared (N^2) divided by the diffusion constant (N^{-1}). Thus a backbone segment of order N requires a time scale $N^2/N^{-1}=N^3$ to be renewed (this in fact explains the reptation exponent $z=3$). On the other hand, to change that backbone segment by direct hopping over barriers, one needs the time N/c. The fastest process dominates and the competition is controlled by the ratio of the rates $N^3/(N/c)=cN^2$. So the crossover scaling function should be a function of the ratio cN^2, which yields $\theta=1/2$.

One may wonder why it is so difficult for DMRG to reach long N for small c, while the Hamiltonian simplifies for $c=0$. As one observes from Figs. 7 and 8, there is a zone where the values make a turn from reptative behavior to Rouse dynamics. The basis in the DMRG approximation has to be large enough to notice this difference in behavior at the appropriate N, which grows as $c^{-1/2}$. One needs a basis size m of the same order to describe the crossover. It does not mean that it is impossible to use DMRG for the pure cage model with $c=0$. But then one has to use a representation of the Hamiltonian which explicitly acknowledges the extra symmetries which are present in this model. Additional symmetries of the cage model are discussed in the papers of van Heukelum *et al.* [9]. A similar situation occurs in crossover in the Rubinstein-Duke model [19].

The results of this paper are quite similar to the crossover found in a one-dimensional Rubinstein-Duke model with hernia creation and annihilation [16]. This leads us to believe that the crossover in gels is a universal phenomenon with the crossover exponent $\theta=1/2$, independent of the embedding lattice, as long as the embedding lattice permits sideways motion, which cross the barriers. Sometimes the motion rules exclude crossing of barriers, e.g., in the one-dimensional embedding. But also in a lattice with triangular cells, crossing is

impossible within the rule that links are always between nearest neighbor cells.

We find that with fixed nonzero crossing rate c, the chain always tends towards Rouse dynamics for larger and larger N. This contrasts the general observation that in polymer melts the opposite tendency takes place: longer chains display reptative behavior [6,20]. It is clear that the obstruction due to other polymers cannot be seen as a fixed barrier, with a certain tunneling rate. Thus our results cannot be applied to polymer melts using a fixed rate for sideways motion. In other words, c must become a function of the chain length. To handle a chain length dependent Hamiltonian gives a complication in DMRG. Apart from the difficulties to find an adequate model for polymer melts that allows one to treat very long chains accurately, we may speculate that an "effective" rate c for sideways motion depends as a power $N^{-\alpha}$ on the length N. The combination $cN^2 \sim N^{2-\alpha}$ determines whether one sees reptation of Rouse dynamics. It is tempting to take for α the effective renewal exponent z_N, defined in Eq. (12), because it takes the renewal time for a polymer to move out of the way. As this α is always larger than 2, the combination shrinks with growing length, making the α even larger. Thus one observes the opposite crossover: from Rouse dynamics to reptation.

Although it is feasible to realize experimentally two-dimensional systems, we do not think that it is of great importance to discuss these possibilities, since our results are likely not very sensitive to the dimensionality of the system. The universal quantities that we calculate apply also to three-dimensional systems.

ACKNOWLEDGMENTS

The authors thank Gerard Barkema for most stimulating discussions.

[1] P. G. de Gennes, *Scaling Concepts in Polymer Physics* (Cornell University Press, Ithaca, NY, 1971).
[2] K. E. Evans and S. F. Edwards, J. Chem. Soc., Faraday Trans. 2 **77**, 1891 (1981); **77**, 1913 (1981); **77**, 1929 (1981).
[3] J.-L. Viovy, Rev. Mod. Phys. **72**, 813 (2000).
[4] J. Klein Wolterink and G. T. Barkema, Mol. Phys. **103**, 3083 (2005).
[5] J. M. Deutsch, Phys. Rev. Lett. **49**, 926 (1982).
[6] Kurt Kremer, Gary S. Grest, and I. Carmesin, Phys. Rev. Lett. **61**, 566 (1988).
[7] J. Reiter, J. Chem. Phys. **94**, 3222 (1991).
[8] G. T. Barkema and H. M. Krenzlin, J. Chem. Phys. **109**, 6486 (1998).
[9] A. van Heukelum and H. R. W. Beljaars, J. Chem. Phys. **113**, 3909 (2000); A. van Heukelum and G. T. Barkema, Electrophoresis **23**, 2562 (2002); A. van Heukelum, G. T. Barkema, and R. H. Bisseling, J. Comput. Phys. **180**, 313 (2002).
[10] S. R. White, Phys. Rev. Lett. **69**, 2863 (1992); U. Schollwoeck, Rev. Mod. Phys. **77**, 259 (2005).
[11] L. Schäfer, U. Ebert, and A. Baumgartner, Phys. Rev. E **65**, 061505 (2002).
[12] One could rename B^2, to B, but this might give confusion with respect to the convention in the Rubenstein-Duke model, where moves with bias B are allowed.
[13] B. Derrida, M. Evans, V. Hakim, and V. Paquier, J. Phys. A **26**, 1493 (1993).
[14] T. Sasamoto, J. Phys. A **32**, 7109 (1999).
[15] R. A. Blythe, M. R. Evans, F. Colaiori, and F. H. L. Essler, J. Phys. A **33**, 2313 (2000).
[16] A. Drzewiński and J. M. J. van Leeuwen, Phys. Rev. E **73**, 051801 (2006); A. Buhot, Eur. Phys. J. E **18**, 239 (2005).
[17] E. Carlon, A. Drzewiński, and J. M. J. van Leeuwen, J. Chem. Phys. **117**, 2435 (2002).
[18] E. Carlon, A. Drzewiński, and J. M. J. van Leeuwen, Phys. Rev. E **64**, 010801(R) (2001).
[19] A. Drzewiński and J. M. J. van Leeuwen (unpublished).
[20] A. Wischnewski, M. Monkenbusch, L. Willner, D. Richter, and G. Kali, Phys. Rev. Lett. **90**, 058302 (2003).